Paper

New Research on AC–AC Converters without Intermediate Storage and Their Applications in Power-Electronic Transformers and AC Drives

Krushna Keshab Mohapatra*, Non-member
Ranjan Gupta*, Non-member
Satish Thuta**, Non-member
Apurva Somani*, Non-member
Amod Umarikar*, Non-member
Kaushik Basu*, Non-member
Ned Mohan*a, Non-member

AC-AC converters (e.g. matrix converters) are mostly semiconductor solutions for applications where intermediate energy storage is eliminated. This paper summarizes the research done and being carried out at the University of Minnesota for applications in motor drives and power-electronic transformers with advanced features. This paper presents a carrier-based modulation method for matrix converters and its application during for both input unbalance and output over-modulation. Various topologies of matrix converter are described for both drives and power-electronic transformers. These topologies have some inherent benefits like common-mode voltage elimination across the bearings of the motor/generator and controllable power factor at the input side. Some of the described technologies require open-ended machines as load and thereby some advantages like enhanced output voltage (1.5 times the output of normal three terminal load) are achieved. © 2009 Institute of Electrical Engineers of Japan. Published by John Wiley & Sons, Inc.

1. Introduction

Matrix converter is a converter topology which has the least number of passive components compared to conventional converter topologies [1–4]. It uses only semiconductor switches for power conversion objectives without any intermediate energy storage. It basically consists of nine four-quadrant switches, which connects the three-phase input to the three-phase output (Fig. 1) [5]. Matrix converter has also an added advantage of input and output power factor decoupling.

Various modulation schemes for matrix converters are described in the literature, which require addition of the harmonics of the output frequency [3,4] and input frequency to the modulation indices, and require sector information for generation of PWM signals [4–8]. A simple modulation method is presented in Ref. 9, which neither needs any sector information nor any harmonic injection for calculation of the duty ratios. Also the output voltage is synthesized to its maximum capacity without compromising any benefits of the conventional techniques [4–8]. The modulation method is also extended for an unbalance condition at input and over-modulation at the output [10,11].

The open-ended three-phase drive systems are obtained by opening the stator winding neutral of the three-phase motor and driving the motor from both sides of the stator winding using two inverters [12–15]. By doing so, the output voltage is enhanced and the DC-link voltage requirement is reduced. Generally, in the previous works, normal two-level and multi-level inverters are used for the open-ended winding. In the proposed system, the motor is driven from two matrix converters which are connected to the opposite sides of the open-end winding. Although the proposed topology is available in scene since long time [1,2,16,17] called 36-switch unrestricted frequency changer, a space vector modulation technique is developed for the control of the converter with power factor control in entire range [18]. Common-mode voltage elimination from a single matrix converter driven drive is described in Ref. 19 by using Venturini's first method. The control by default eliminates any common-mode voltage at the load terminals. An alternate 36-switch indirect topology is also described [20] which has some advantages like reduced switching loss, reduced clamp circuit requirement and better commutation. Both of the techniques use large number of switches which increases the switching loss, cost and volume of the system. A reduced switch count matrix converter driven open-ended load topology is proposed which is quite simple from both design and operation perspective [21].

In electrical power applications transformers occupy a large volume in terms of space and cost. Mostly in high power adjustable speed AC drives with flexible voltage transfer ratio, there is often a bulky low frequency transformer at the input for isolation. The transformers occupy a large volume in the overall drive system. The larger volume and weight of transformer mostly comes from low line frequency (50/60 Hz) excitation. Thus, by increasing the excitation frequency by means of power converter systems, the transformer size can be reduced to a large extent. Different topologies of both DC links based and matrix converter based power-electronic transformers are available in literature [22–27]. In this paper, different topologies of matrix converter based power-electronic transformers are investigated. In one of the topologies, a three-phase to one-phase matrix converter with high frequency

---
a Correspondence to: Ned Mohan. E-mail: mohan@umn.edu

* Department of Electrical and Computer Engineering, University of Minnesota, Minneapolis, 200, Union Street, SE, Minneapolis, MN 55455, USA
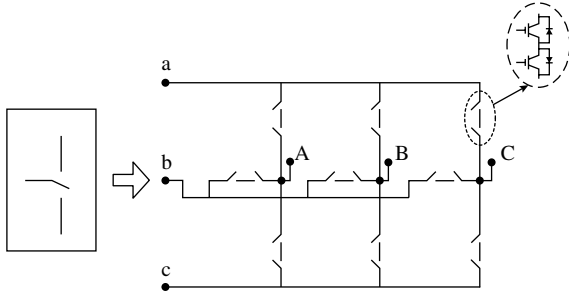** Ford Motors, MI, USA
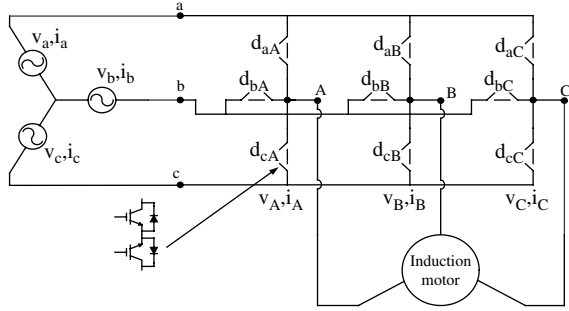
Fig. 1. Nine switch matrix converter

Fig. 2. Matrix converter driven three-phase machine

transformer is used for common-mode elimination at the output [28]. Another topology uses three direct matrix converters with primary of the transformer open for generation high frequency transformer application [29].

2. Simplified Matrix Converter Modulation Strategy

A simple three-phase to three-phase matrix converter can be treated as a three-level inverter. In three-level converters [30], the input DC voltage takes on one of the three DC values: V_d+, 0, V_d-. But in matrix converters, the input voltages are three-phase AC. In three-level inverters, in a switching period, the output voltage is synthesized by using the nearest available voltage levels, but in matrix converter the output voltage is generated by using all available three levels, thereby ensuring power factor control at the input.

Thus, any output phase is connected to all three input phases in a switching period for some interval determined by the corresponding duty ratios. The input phase voltages v_a, v_b, v_c and the output phase voltages v_A, v_B, v_C are related by the relation shown in (1). The duty ratio for each switch connecting between input and output is shown in Fig. 2.

Similarly, the input current i_a, i_b, i_c and the output current i_A, i_B, i_C are related by (2).

$$\begin{bmatrix} v_A \\ v_B \\ v_C \end{bmatrix} = \begin{bmatrix} d_{aA} & d_{bA} & d_{cA} \\ d_{aB} & d_{bB} & d_{cB} \\ d_{aC} & d_{bC} & d_{cC} \end{bmatrix} \times \begin{bmatrix} v_{an} \\ v_{bn} \\ v_{cn} \end{bmatrix} \quad (1)$$

$$\begin{bmatrix} i_a \\ i_b \\ i_c \end{bmatrix} = \begin{bmatrix} d_{aA} & d_{aB} & d_{aC} \\ d_{bA} & d_{bB} & d_{bC} \\ d_{cA} & d_{cB} & d_{cC} \end{bmatrix} \times \begin{bmatrix} i_A \\ i_B \\ i_C \end{bmatrix} \quad (2)$$

Thus, the matrix converter can be represented by a equivalent circuit which comprises of variable turns ratio transformers as shown in Fig. 3. The duty ratios of the matrix converter represent the turns ratio of the transformers. The input is three-phase sinusoidal in nature, i.e. $v_a = \hat{V} \cos(\omega t)$, $v_b = \hat{V} \cos(\omega t - 2\pi/3)$, $v_c = \hat{V} \cos(\omega t - 4\pi/3)$. Therefore, the duty ratios shown in (1) and (2) are sinusoidal in nature for the elimination of input frequency terms from the output. Equation 3 shows the duty ratios
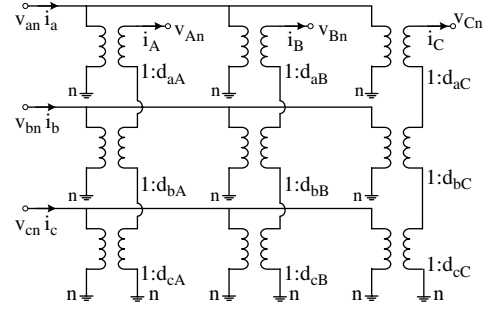

Fig. 3. Equivalent circuit representation of matrix converter

for output phase-A where $k_A(t)$ denotes the output amplitude control term and ρ denotes the input power factor control term.

$$\begin{bmatrix} d_{aA} \\ d_{bA} \\ d_{cA} \end{bmatrix} = \begin{bmatrix} k_A(t) \cos(\omega t - \rho) \\ k_A(t) \cos(\omega t - 2\pi/3 - \rho) \\ k_A(t) \cos(\omega t + 2\pi/3 - \rho) \end{bmatrix} \quad (3)$$

2.1. Offset duty ratio At any instant, the condition '$0 <$ (*duty ratio of the switch*) < 1' should be valid. In order to cancel the effect of negative duty ratios, some duty ratios with positive values need to be added to all the output phases in equal proportion so that they only generate finite common-mode voltage at the output without affecting the output line to line voltage.

Considering the case of output phase-A in order to cancel any negative duty ratio from (3), the absolute value of the duty ratio can be added. Thus, the individual offset duty ratios should be

$$\begin{bmatrix} D_a \\ D_b \\ D_c \end{bmatrix} = \begin{bmatrix} |k_A(t) \cos(\omega t - \rho)| \\ |k_A(t) \cos(\omega t - 2\pi 3 - \rho)| \\ |k_A(t) \cos(\omega t + 2\pi 3 - \rho)| \end{bmatrix} \quad (4)$$

The new net duty ratios are $[D_a + d_{aA} \quad D_b + d_{bA} \quad D_c + d_{cA}]^T$. For example, in input phase-a

$$0 < D_a + d_{aA} < 1$$

i.e.

$$0 < |k_A(t)\hat{V} \cos(\omega t - \rho)| + k_A(t)\hat{V} \cos(\omega t - \rho) < 1 \quad (5)$$

This implies that in the worst begin

$$0 < 2|k_A(t)| < 1 \quad (6)$$

which implies the maximum value of $|k_A(t)|$ is 0.5. Hence, the offset duty ratios (Fig. 4) corresponding to the three input phases are chosen as

$$\begin{bmatrix} D_a \\ D_b \\ D_c \end{bmatrix} = \begin{bmatrix} |0.5 \cos(\omega t - \rho)| \\ |0.5 \cos(\omega t - 2\pi 3 - \rho)| \\ |0.5 \cos(\omega t + 2\pi 3 - \rho)| \end{bmatrix} \quad (7)$$
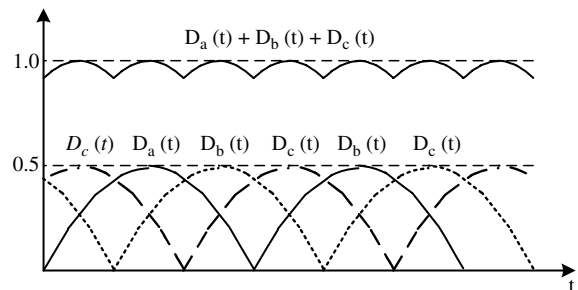

Fig. 4. The offset duty ratios corresponding to all input phases drawn for a particular case

592

To utilize three-phase output generation to full capacity, an additional common-mode term V_{COM} equal to $\{[\max(k_A(t), k_B(t), k_C(t)) + \min(k_A(t), k_B(t), k_C(t))]/2\}$ is added [10] according to the traditional space vector PWM principle. Thus, the amplitude of $k_A(t), k_B(t), k_C(t)$ can be enhanced from 0.5 to 0.57 and the output amplitude is equal to $(\sqrt{3}/2)\,\hat{V}\cos\rho = 0.866\,\hat{V}\cos\rho$.

$$\begin{bmatrix} d_{aA} \\ d_{bA} \\ d_{cA} \end{bmatrix} = \begin{bmatrix} D_a + [k_A(t) - V_{COM}]\cos(\omega t - \rho) \\ D_b + [k_A(t) - V_{COM}]\cos(\omega t - 2\pi 3 - \rho) \\ D_c + [k_A(t) - V_{COM}]\cos(\omega t + 2\pi 3 - \rho) \end{bmatrix} \tag{8}$$

But the summation $[D_a(t) + D_b(t) + D_c(t)]$ is less than or equal to unity as shown in Fig. 4. Therefore, in order to make the summation equal to unity another offset duty ratio $\Delta(t)$ equal to $[(1 — (D_a(t) + D_b(t) + D_c(t)))/3]$ is added to the original value of $D_a(t), D_b(t)$ and $D_c(t)$ in (8). This scheme is easy for implementation and it neither requires any look up table nor any harmonic injection in the modulating signal.

3. Matrix Converter Over-Modulation

Similar to over-modulation in normal converters, matrix converter can be operated in over-modulation mode to increase the fundamental output with some additional harmonics. But there are multiple over-modulation modes in matrix converter, because both the output voltage and input voltage are sinusoidal AC. The types of over-modulation modes are

1. Output-side over-modulation.
2. Input-side over-modulation with power factor control.
3. Input-side over-modulation without power factor control.
4. Simultaneous input- and output-side over-modulation.

3.1. Output-side over-modulation The matrix converter can be made to operate in this mode by increasing the amplitude of the reference output voltage modulating signals $k_A(t), k_B(t), k_C(t)$ above the maximum values which is equal to 0.57. In this condition, for a fictitious DC-link voltage of magnitude V_{dc_fict}, the peak fundamental amplitude of the output phase voltage can be found to be $2V_{dc\_fict}/\pi$. The magnitude of this fictitious DC-link voltage, in linear modulation region, in the matrix converter depends on the peak input voltage amplitude, the power factor of the input currents and can be computed as $V_{dc\_fict} = (3/2)\hat{V}\cos\rho$.

Thus, with input unity power factor, the peak fundamental output phase voltage $\hat{V}_o$ can be given as

$$\hat{V}_o = 2V_{dc\_fict}/\pi = 0.95\hat{V} \tag{9}$$

The gain of the modulation in the over-modulation region is a nonlinear function of the peak amplitude of the reference modulating signal [31]. At maximum output over-modulation (i.e. six-step square wave mode), all the instantaneous output references (i.e. $k_A(t) - V_{COM}$ for phase-A) (8) are clipped to the value ± 0.5. With the choice of reference modulating signals in (8) discussed in the previous section, the true square wave mode (square wave duty ratios) occurs for peak amplitudes.

3.2. Input over-modulation with power factor control The idea in this over-modulation mode is to increase the fictitious DC-link voltage by reducing the offset duty-ratio $\Delta(t)$ as shown in (10). To achieve this, the choice of the input duty ratios should be modified such that they sum to unity in a switching cycle with
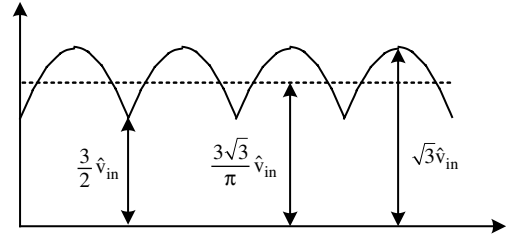

Fig. 5. DC-link voltage of a diode bridge converter supplying a resistive load

reduced offset duty-ratio $\Delta(t)$.

$$\begin{bmatrix} d_{aA} \\ d_{bA} \\ d_{cA} \end{bmatrix} = \begin{bmatrix} D_a + [k_A(t) - V_{COM}]\cos(\omega t - \rho) + \Delta(t) \\ D_b + [k_A(t) - V_{COM}]\cos(\omega t - 2\pi 3 - \rho) + \Delta(t) \\ D_c + [k_A(t) - V_{COM}]\cos(\omega t + 2\pi 3 - \rho) + \Delta(t) \end{bmatrix} \tag{10}$$

In order to utilize the offset duty-ratio period $\Delta(t)$ for over-modulation, the other duty ratios in (10) must be scaled up in same proportion such that they sum to unity. Thus the modified duty ratios are as shown in (11)

$$\begin{bmatrix} d_{aA}^o \\ d_{bA}^o \\ d_{cA}^o \end{bmatrix} = \frac{1}{1 - 3 \times \Delta(t)} \times \begin{bmatrix} D_a + [k_A(t) - V_{COM}]\cos(\omega t - \rho) \\ D_b + [k_A(t) - V_{COM}]\cos(\omega t - 2\pi 3 - \rho) \\ D_c + [k_A(t) - V_{COM}]\cos(\omega t + 2\pi 3 - \rho) \end{bmatrix} \tag{11}$$

3.3. Input over-modulation without power factor control In this scheme, a different approach to input-side over-modulation achieves the highest possible output voltage of the converter. Using this method, the fictitious DC-link voltage can be increased to the theoretical maximum value as shown by the dotted line in Fig. 5 which is equivalent to the output of three-phase diode bridge rectifier.

In such a case, the input over-modulation described in the previous section becomes a special case of the generalized method in which the time varying functions are all the same.

3.4. Simultaneous input- and output-side over-modulation The modifications to the duty ratios for input over-modulation do not affect the choice of the reference output voltage modulating signals. Thus, the matrix converter can be operated in the over-modulation region with simultaneous input- and output-side over-modulation. With the input duty ratios chosen as in (11) and by increasing the peak amplitude of the reference output voltage modulating signal in square wave mode, the output to input voltage transfer ratio can be increased to unity when the input power factor is unity as shown in (12).

$$V_O = \frac{2V_{dc\_fict}^o}{\pi} = \frac{2 \times 1.049}{\pi}V\cos\rho = 1.001\,V\cos\rho \tag{12}$$

With input-side over-modulation without power factor control and the output side in square wave mode the input–output transfer ratio can be taken above unity as shown in (13).

$$V_O = \frac{2V_{dc\_fict}^o}{\pi} = \frac{6\sqrt{3}}{\pi^2}V = 1.053\,V \tag{13}$$

4. Extension of the Carrier-Based Pwm Scheme for Operation Under Unbalanced Input Voltages

Neglecting the switching losses, the power at the input current port is equal to the power at the output voltage port of a matrix

converter due to the absence of any energy storage element in-between. When there is an unbalance in the input voltages, one has to compromise between balancing and/or the sinusoidal nature, either in the input-side currents or in the output-side voltages, so as to satisfy the power transfer condition. In this regard, three such techniques which use space vectors for output voltage generation are extended for application with the presented modulation technique [32–35]. In method-1, the input currents are sinusoidal but are unbalanced, whereas in method-2 and -3 sinusoidal currents with additional harmonics are in the input side. Any unbalanced set of three-phase voltages can be represented as the sum of positive and negative sequence components.

$$v_{a_P} = \hat{V}_P \cos(\omega_i t + \varphi_p), v_{a_N} = \hat{V}_N \cos(\omega_i t + \varphi_N) \quad (14)$$

$$v_{b_P} = \hat{V}_P \cos(\omega_i t - 2\pi/3 + \varphi_P),$$

$$v_{b_N} = \hat{V}_N \cos(\omega_i t + 2\pi/3 + \varphi_N) \quad (15)$$

$$v_{c_P} = \hat{V}_P \cos(\omega_i t + 2\pi/3 + \varphi_P),$$

$$v_{c_N} = \hat{V}_N \cos(\omega_i t - 2\pi/3 + \varphi_N) \quad (16)$$

Thus, $v_a = v_{a_P} + v_{a_N}$, $v_b = v_{b_P} + v_{b_N}$ and $v_c = v_{c_P} + v_{c_N}$, where $(\hat{V}_P, \varphi_p)$ and $(\hat{V}_N, \varphi_N)$ are the amplitude and phase of the positive and negative sequence voltages respectively. The zero sequence voltages are absent in a three-wire system.

4.1. Method-1

The modulation indices for the switches corresponding to any output phase in this method are generated from the positive and negative sequence components of the input voltage. The duty ratios (i.e d_{aA}, d_{bA}, d_{cA} for phase-A) have positive sequence $(d_{aA_P}, d_{bA_P}, d_{cA_P})$ and negative sequence $(d_{aA_N}, d_{bA_N}, d_{cA_N})$ components in proper ratio (18) and (19)) in order to make the output voltages balanced.

$$d_{aA} = d_{aA_P} + d_{aA_N}, d_{bA} = d_{bA_P} + d_{bA_N}, d_{cA} = d_{cA_P} + d_{cA_N}$$
$$(17)$$

$$\begin{bmatrix} d_{aA_P} \\ d_{bA_P} \\ d_{cA_P} \end{bmatrix} = k_{A_P} \begin{bmatrix} \cos(\omega_i t + \varphi_P) \\ \cos(\omega_i t - 2\pi/3 + \varphi_P) \\ \cos(\omega_i t + 2\pi/3 + \varphi_P) \end{bmatrix}$$
$$(18)$$

$$\begin{bmatrix} d_{aA_N} \\ d_{bA_N} \\ d_{cA_N} \end{bmatrix} = -k_{A_N} \begin{bmatrix} \cos(\omega_i t + \varphi_N) \\ \cos(\omega_i t + 2\pi/3 + \varphi_N) \\ \cos(\omega_i t - 2\pi/3 + \varphi_N) \end{bmatrix}$$
$$(19)$$

In order to eliminate any harmonic terms from the output k_{A_P} and k_{A_N} are chosen in proportion to the input positive sequence and negative sequence voltages.

$$k_{A_P} = k\hat{V}_P, k_{A_N} = k\hat{V}_N \quad (20)$$

Where 'k' is proportional to the instantaneous modulation index of the output phase-A. From (14) to (19) the maximum and minimum limits of 'k' can be obtained as $-0.5/(\hat{V}_P + \hat{V}_N) \le k \le 0.5/(\hat{V}_P + \hat{V}_N)$. Thus, the range of variation of phase-A voltage can be calculated as in (12).

In order to compensate for the unrealizable negative duty ratios, the offset duty ratios shown in (13)–(15) are added [10].

$$D_A = \left| \frac{0.5\hat{V}_P}{\hat{V}_P + \hat{V}_N} \cos(\omega_i t + \varphi_P + \rho_P) \right|$$

$$+ \left| \frac{0.5\hat{V}_N}{\hat{V}_P + \hat{V}_N} \cos(\omega_i t + \varphi_N + \rho_P) \right| \quad (21)$$

$$D_B = \left| \frac{0.5\hat{V}_P}{\hat{V}_P + \hat{V}_N} \cos(\omega_i t - 2\pi/3 + \varphi_P + \rho_P) \right|$$

$$+ \left| \frac{0.5\hat{V}_N}{\hat{V}_P + \hat{V}_N} \cos(\omega_i t + 2\pi/3 + \varphi_N + \rho_P) \right| \quad (22)$$

$$D_C = \left| \frac{0.5\hat{V}_P}{\hat{V}_P + \hat{V}_N} \cos(\omega t + 2\pi/3 + \varphi_P + \rho_P) \right|$$

$$+ \left| \frac{0.5\hat{V}_N}{\hat{V}_P + \hat{V}_N} \cos(\omega t - 2\pi/3 + \varphi_N + \rho_P) \right| \quad (23)$$

4.2. Method-2

Using three phase to stationary two-phase transformation, the unbalanced input voltages result in the tip of the resultant voltage-vector rotating in an elliptical trajectory as shown in Fig. 6. The instantaneous amplitude and the phase of the resultant vector are as follows:

$$V_{inst} = \sqrt{\hat{V}_P^2 + \hat{V}_N^2 + 2\hat{V}_P \hat{V}_N \cos(2\omega_i t + \varphi_P + \varphi_N)} \quad (24)$$

$$\theta_{inst} = \tan^{-1} \frac{(\hat{V}_P \sin(\omega t + \varphi_P) - \hat{V}_N \sin(\omega t + \varphi_N))}{(\hat{V}_P \cos(\omega t + \varphi_P) + \hat{V}_N \cos(\omega t + \varphi_N))} \quad (25)$$

The instantaneous modulation indices in this method are calculated based on the amplitudes of the resultant and reference voltage vectors. The amplitude of the reference voltage vector is $(\hat{V}_P - \hat{V}_N)$, which is equal to the amplitude of the minor axis of the ellipse. The vectors are shown as dotted lines in Fig. 6. Hence, the maximum amplitude of the modulation index at any instant to make the output voltage balanced is $(\hat{V}_P - \hat{V}_N)/V_{inst}$.

Taking the case of output phase-A, the duty ratios for the switches corresponding to input phase-a, b, c are chosen as follows, where ρ is the desired input power factor and k_A is the output modulation index:

$$d_{aA} = k_A \frac{|(\hat{V}_P - \hat{V}_N)|}{V_{inst}} \cos(\omega_{inst} t + \rho)$$

$$d_{bA} = k_A \frac{|(\hat{V}_P - \hat{V}_N)|}{V_{inst}} \cos(\omega_{inst} t - 2\pi/3 + \rho) \quad (26)$$

$$d_{cA} = k_A \frac{|(\hat{V}_P - \hat{V}_N)|}{V_{inst}} \cos(\omega_{inst} t + 2\pi/3 + \rho)$$

$$D_A = |0.5 \cos(\omega_{inst} t + \rho)|$$

$$D_B = |0.5 \cos(\omega_{inst} t - 2\pi/3 + \rho)| \quad (27)$$

$$D_C = |0.5 \cos(\omega_{inst} t + 2\pi/3 + \rho)|$$

The instantaneous voltage-vector magnitude can be obtained by stationarily transforming the input three-phase voltages. To
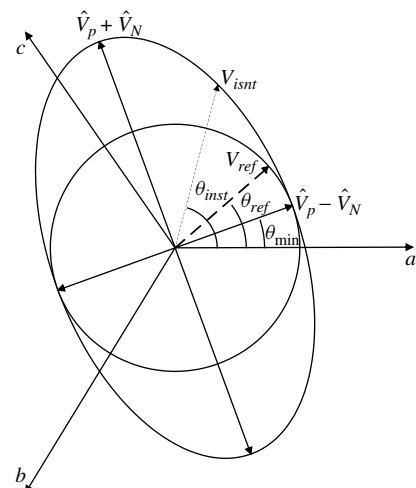

Fig. 6. Instantaneous voltage vectors

compensate for the negative duty ratios, offset duty ratios shown in (27) is desired.

4.3. Method-3 The instantaneous modulation indices are calculated based on both the amplitude and the phase of the resultant and reference voltage vectors. The amplitude of the reference voltage vector is $(\hat{V}_P - \hat{V}_N)$, which is equal to the amplitude of the minor axis of the ellipse and rotates at an angular speed equal to the input frequency, implying that the phase of the reference vector (θ_{ref}) at any instant is the same as $(\omega_i t + \varphi_P)$ of the positive-sequence input voltage. The vectors are shown as dotted lines in Fig.6. Hence, the maximum amplitude of the modulation index at any instant to make the output voltage balanced is $\frac{(\hat{V}_P - \hat{V}_N)}{V_{\text{inst}} \cos(\theta_{\text{inst}} - \theta_{\text{ref}})}$.

Taking the case of the output phase-A, the duty ratios for the switches corresponding to input phase- a, b, c are chosen as

$$d_{aA} = k_A \frac{(\hat{V}_P - \hat{V}_N)}{V_{\text{inst}} \cos(\theta_{\text{inst}} - \theta_{\text{ref}})} \cos(\theta_{\text{ref}} + \rho)$$

$$d_{bA} = k_A \frac{(\hat{V}_P - \hat{V}_N)}{V_{\text{inst}} \cos(\theta_{\text{inst}} - \theta_{\text{ref}})} \cos(\theta_{\text{ref}} - 2\pi/3 + \rho) \quad (28)$$

$$d_{cA} = k_A \frac{(\hat{V}_P - \hat{V}_N)}{V_{\text{inst}} \cos(\theta_{\text{inst}} - \theta_{\text{ref}})} \cos(\theta_{\text{ref}} + 2\pi/3 + \rho)$$

And for cancellation of negative duty ratios the corresponding offset duty ratios are shown in (29),

$$D_A = |0.5 \cos(\theta_{\text{ref}} + \rho)|$$
$$D_B = |0.5 \cos(\theta_{\text{ref}} - 2\pi/3 + \rho)| \quad (29)$$
$$D_C = |0.5 \cos(\theta_{\text{ref}} + 2\pi/3 + \rho)|$$

To make the sum of duty ratios in a switching period equal to one, another offset duty ratio equal to $\{1 - (D_A + D_B + D_C)\}/3$ is invariably added to the original duty ratios in all the three methods.

5. Open-End Winding Three-Phase Matrix Converter Drive

In open-ended three-phase motor drive, the stator neutral of the machine is opened and is connected with another set of supply (Fig. 7 [12–20]). In consequence, the stator is excited from two inverters from both ends, thus enabling large voltage rated motors to be driven from inverters of lower voltage rating. The inverters in the open-end drive can be replaced by matrix converters, which is generally known as 18-switch unrestricted frequency changer [1,2].
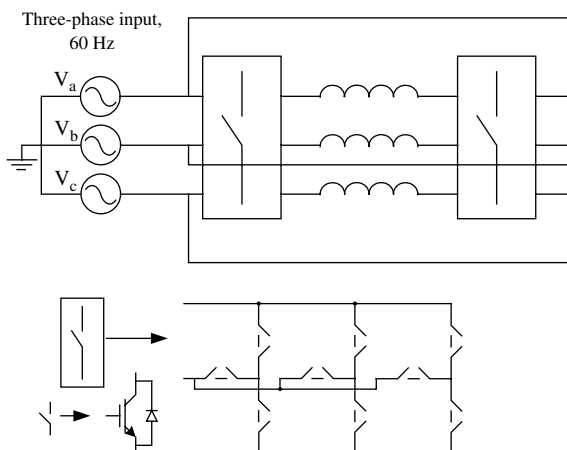

Fig. 7. Direct matrix converter base open-end winding drive

The topologies and control are such that input phase voltages are connected to two sets of output phase voltage at the terminals of a motor/generator. This is done by solid-state switches (without energy storage capacitors and inductors) such that all currents at the two sets of output phase terminals always have paths to flow to the input phase voltages [20]. The maximum motor voltage capability is 1.5 per unit (pu), that is, $V_{\text{ph,m}} = 1.5V_{\text{ph,in}}$ where $V_{\text{ph,m}}$ is the output motor phase voltage and $V_{\text{ph,in}}$ is the input phase voltage and also eliminates the common-mode voltages at both ends. At the same time, the insulation stress is equal to the magnitude of input phase voltage only.

For a single matrix converter, the input phases-a, b, c are connected to the output phases-A, B, C through switching scheme shown in Table I. This results in null common-mode voltages at the output [18,19]. There are six possible combinations and they can be divided into two sub-groups. The first sub-group using abc, cab and bca as shown in Fig. 8 (top), results in counterclockwise (CCW) rotating vectors and the second sub-group using acb, bac and cba results in clockwise (CW) rotating vectors. Both sets of vectors synthesize the resultant output voltage limited to maximum amplitude of 0.5 times the input voltage [18].

When the machine is driven by two matrix converters as shown in Fig. 7, the net output voltage is the vector addition of voltages from individual matrix converters. Using CCW rotating vectors from both matrix converters, six CCW rotating active vectors and three zero vectors are generated [18]. Similarly, CW vectors from both matrix converters results in another set of six CW rotating voltage vectors and three zero vectors. The amplitude of the resultant voltage vector generated by combining the voltage vectors of both converters equals ($1.732 \times 3/2V$).
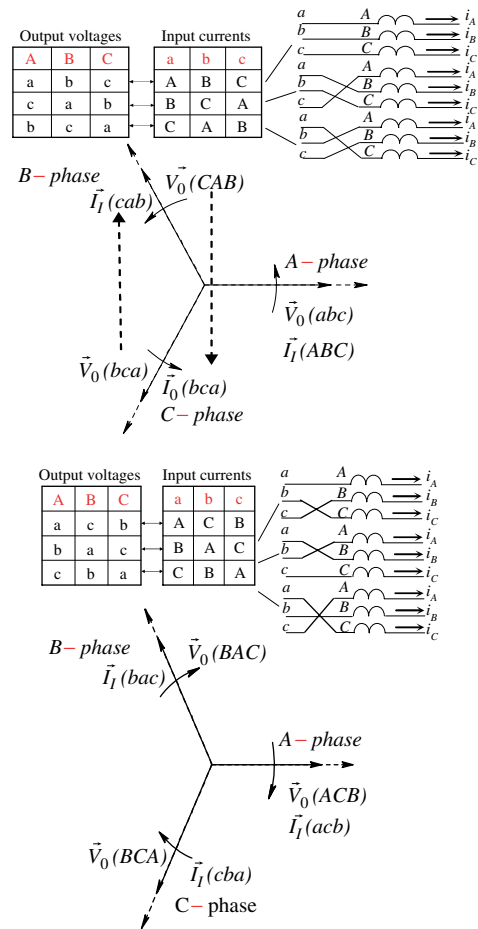

Fig. 8. Utility side power factor using CCW vectors (top) and CW vectors

Table I. Switching combination for zero CMV

ABC	V_{AB}	V_{BC}	V_{CA}	V_{COM}
abc	v_{ab}	v_{bc}	v_{ca}	0
acb	$-v_{ca}$	$-v_{bc}$	$-v_{ab}$	0
bca	v_{bc}	v_{ca}	v_{ab}	0
bac	$-v_{ab}$	$-v_{ca}$	$-v_{bc}$	0
cab	v_{ca}	v_{ab}	v_{bc}	0
cba	$-v_{bc}$	$-v_{ab}$	$-v_{ca}$	0

5.1. Utility side power factor control As described in previous section, the switching combinations (abc, cab and bca) and (acb, bac and cba) generate anticlockwise and clockwise rotating vectors at the output respectively. The resultant output voltage vector constructed from the two switching sets can be either anticlockwise or clockwise, which consequently generates corresponding anticlockwise or clockwise rotating resultant output current vector. The output voltage vector can be represented in terms of the input voltage vector and switching vector. Similarly the input current vector can be represented in terms of the output current vector. Figure 8 illustrates voltages and currents, where the lower case letters (a, b and c) are used to designate voltages and currents at the input side and capital letters (A, B and C) are used to designate output voltages of the converter and output currents flowing in the phase windings of the AC machine.

The input side three-phase voltage represented by anticlockwise rotating voltage vector which is $\hat{V}e^{i\omega t}$, where ω is the input frequency. The switching vectors (abc, cab and bca) transform the input voltage vector to the counterclockwise rotating output vectors. $\hat{V}e^{i\omega t}$, $\hat{V}e^{i(\omega t + 2\pi/3)}$ and $\hat{V}e^{i(\omega t - 2\pi/3)}$, respectively, and switching vectors (acb, bac and cba) transform it to the clockwise rotating output vectors $\hat{V}e^{-i\omega t}$, $\hat{V}e^{i(-\omega t + 2\pi/3)}$ and $\hat{V}e^{i(-\omega t - 2\pi/3)}$, respectively. The time weighted average voltage vector in a switching period results in the resultant output voltage vector $\hat{V}_o e^{i\omega_o t}$ which for example also rotates anticlockwise. The net output voltage vector $\hat{V}_o e^{i\omega_o t}$ is decomposed into two parts $\hat{V}_{o\_ccw}e^{i\omega_o t + k}$ and $\hat{V}_{o\_cw}e^{i\omega_o t - k}$ which are generated from the anticlockwise set $\hat{V}e^{i\omega t}$, $\hat{V}e^{i(\omega t + 2\pi/3)}$ and $\hat{V}e^{i(\omega t - 2\pi/3)}$ and the clockwise rotating vector set $\hat{V}e^{-i\omega t}$, $\hat{V}e^{i(-\omega t + 2\pi/3)}$ and $\hat{V}e^{i(-\omega t - 2\pi/3)}$, respectively.

The output current vector is represented by $\hat{I}_o e^{i\omega_o t - \rho_0}$, where ρ_0 is the output power factor angle. As illustrated in Fig. 8, the switching sequence (abc, cab and bca) at the output side will generate a dual switching sequence (ABC, BCA and CAB) at the input side, which would respectively produce current vector $\hat{I}_O e^{i(\omega_o t - \rho_0)}$, $\hat{I}_O e^{i(\omega_o t - \rho_0 - 2\pi/3)}$ and $\hat{I}_O e^{i(\omega_o t - \rho_0 + 2\pi/3)}$ at input.

Similarly, clockwise set of switching sequence produces input switching sequence (ACB, BAC and CBA) and respective input-side current vectors $\hat{I}_O e^{-i(\omega_o t - \rho_0)}$, $\hat{I}_O e^{i(-\omega_o t + \rho_0 + 2\pi/3)}$ and $\hat{I}_O e^{i(-\omega_o t + \rho_0 - 2\pi/3)}$.

Resultant input current vectors from CCW and CW sequences are given by

$$d_{1\_ccw}\hat{I}_O e^{i(\omega_o t - \rho_0)} + d_{2\_ccw}\hat{I}_O e^{i(\omega_o t - \rho_0 - 2\pi/3)}$$
$$+ d_{3\_ccw}\hat{I}_O e^{i(\omega_o t - \rho_0 + 2\pi/3)} = \hat{I}_{o\_ccw}e^{i(\omega_o t - \rho_0 - \alpha(t))}$$

where $\alpha(t) = (-\omega t + \omega_o t - k)$ (30)

$$\hat{I}_{o\_ccw}e^{i(\omega_o t - \rho_0 - \alpha(t))} = \hat{I}_{o\_ccw}e^{i(\omega_o t - \rho_0 - (-\omega t + \omega_o t - k))}$$
$$= \hat{I}_{o\_ccw}e^{i(\omega t + k - \rho_0)}$$ (31)

$$d_{1cw}\hat{I}_O e^{-i(\omega_o t - \rho_0)} + d_{2cw}\hat{I}_O e^{i(-\omega_o t + \rho_0 + 2\pi/3)}$$
$$+ d_{3cw}\hat{I}_O e^{i(-\omega_o t + \rho_0 - 2\pi/3)} = \hat{I}_{o\_cw}e^{i(-\omega_o t + \rho_0) + \beta(t)}$$

where $\beta(t) = (\omega t + \omega_o t + k)$ (32)

$$\hat{I}_{o\_cw}e^{i(-\omega_o t + \rho_0) + \beta(t)} = \hat{I}_{o\_cw}e^{i(\omega t + \rho_0 + k)}$$ (33)
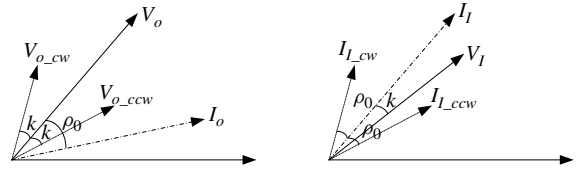

Fig. 9. Relation between input-side power factor and output side power factor

The phasor diagram for both output side and input side are shown in Fig. 9, where the output-side phasors are noted by $V_o = \hat{V}_o e^{i\omega_o t - k}$, $I_o = \hat{I}_o e^{i\omega_o t - \rho_0}$, $V_{o\_ccw} = \hat{V}_{o\_ccw}e^{i\omega_o t - k}$, $V_{o\_cw} = \hat{V}_{o\_cw}e^{i\omega_o t + k}$. The phasors $V_I = \hat{V}e^{i\omega t}$, $I_{I\_ccw} = \hat{I}_{o\_ccw}e^{i(\omega t + k - \rho_0)}$, $I_{I\_cw} = \hat{I}_{o\_cw}e^{i(\omega t + \rho_0 + k)}$ are reflected at the input side. If the reference phasors $\hat{V}_{occw}$ and $\hat{V}_{ocw}$ are equal in both magnitude and phase then by virtue of input–output symmetry, $\hat{I}_{occw}$ and $\hat{I}_{ocw}$ are also of equal in magnitude and phase. If both V_{occw} and V_{ocw} are switched for equal interval then the input phase current I_I has the net phase equal to $((\omega t + \rho_0 + k) + (\omega t - \rho_0 + k))/2 = (\omega t + k)$. Thus by controlling k, the input power factor can be controlled without any influence of output power factor. Similar analysis can be achieved for the other matrix converter which drives the machine from the opposite side and by combining the space phasors from both matrix converters the net output voltage and net input power are controllable.

6. Three-Level Indirect Matrix Converter Based Drive

The three-level indirect matrix converter based open-end drive has several advantages without compromising any functionality of the scheme described in the previous section. This scheme (Fig. 10) has some significant features like less switching and conduction loss and less prone to commutation failure. The topology uses same number of switches as that used in the last section [20]. The converter system constitutes of three three-level inverters. The three-level inverter can be either normal neutral-clamped three-level inverter or any capacitor less three-level inverter. As shown in Fig. 10, the whole inverter system can be divided into two sections. One is the converter section, which converts the three-phase AC to three-level pulsating DC—MAX, MID and MIN which correspond to the maximum, medium and minimum values of the input voltages respectively. The three-phase input is connected to the MAX and the MIN rail through two-quadrant switches and to the MID rail through four-quadrant switches. The other section is the inverter section, which links the output to the pulsating DC link. This section consists of two three-level inverters and each of them is connected to opposite ends of the open-ended load.

The intermediate DC-link waveforms and corresponding space vector are shown in Fig. 11. The voltage waveform at the MAX, MID and MIN rail after rectification are also highlighted. The voltage waveform repeats every $120°$ and the space vector just traverses in the clockwise and anticlockwise direction in only one sector of $60°$.

Any one end of the output section is connected to the pulsating DC link through six possible switching combinations for null common-mode voltage. The switching combinations are divided into two groups (MAX, MID, MIN), (MIN, MAX, MID), (MID, MIN, MAX) and (MAX, MIN, MID), (MID, MAX, MIN) (MIN, MID, MAX). Each group of vectors rotates in the same direction in any sector and both groups rotate in opposite direction. Every consecutive sectors they rotate alternatively CW and CCW. Figure 12 shows one group of vectors (MAX, MID, MIN), (MIN, MAX, MID), (MID, MIN, MAX). The other group will rotate
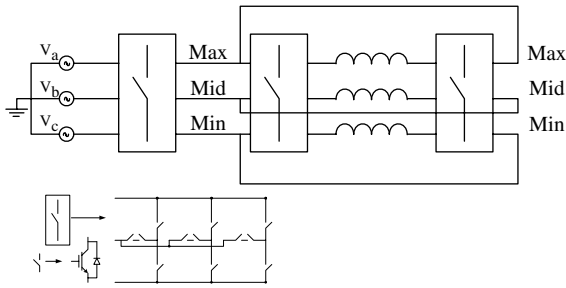
Fig. 10. Three-level indirect matrix converter based open-ended drive
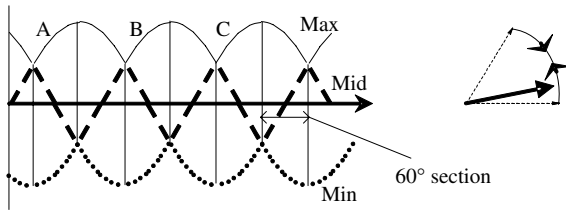

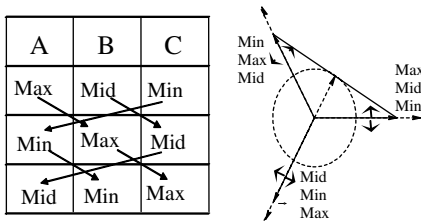Fig. 11. The intermediate DC-link voltages and space

Fig. 12. Space vectors with first group of vector

in opposite direction [20]. These vectors, in either case, can synthesize the output voltage of amplitude equal to 0.5 times the input voltage [18].

By using the space vectors with same rotational direction from both inverters at opposite ends two sets of space vectors are obtained where each set comprises of six hexagonally located space vectors and three null vectors (Fig. 13). The two space sets called reference vector sets rotate in opposite direction at any instant.

The output is generated from either of the two sets of reference space vectors or both by using them alternatively by conventional space vector modulation. The input power factor can be controlled without any influence of output power factor, by using the analysis described in previous sections.

7. Matrix Converter Fed Open-Ended Power-Electronic Transformer For Power System Application

Generally three-phase transformers are used for voltage and current transformation in power transmission and distribution systems. They are large in volume and weight, in terms of copper and iron. Because of large volume they have also large copper and iron loss. Because at line frequency, the core cross section is large in order to generate large flux linkage. If the frequency of the excitation is increased the core cross-section area will be reduced by order of magnitude [22,27]. In order to generate high frequency excitation matrix converters are used, which converts the line frequency input to high frequency voltage by virtue of four-quadrant AC-switches [22–27].

In the present system, two matrix converters drive the open-ended three-phase transformer primary and the star connected
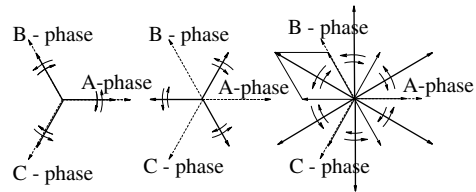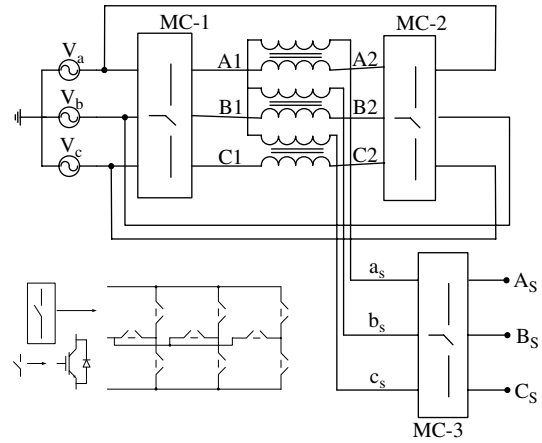

Fig. 13. Output vectors from both inverters of open-end

Fig. 14. Matrix converter fed open-ended power-electronics transformer

Table II. Switching vectors

AA'	BB'	CC'	A_s	B_s	C_s
ab	bc	ca	a_s	b_s	c_s
aa	bb	cc	c_s	a_s	b_s
ba	cb	ac	c_s	a_s	b_s

secondary of the transformer is connected to another matrix converter (Fig.14). The two matrix converters (MC-1 and MC-2) connected to the some source is switched in synchronization in order to generate null common-mode voltage and to produce high frequency AC at the primary windings. Clockwise and anticlockwise switching vectors are switched alternatively with appropriate phase-shift for power factor control [18,20]. The high frequency output at the transformer secondary is reconstructed back to line frequency output by a third matrix converter (MC-3). As discussed in previous section, the amplitude of the basic vectors across the windings, herein the transformer primary winding, is $\sqrt{3}$ pu. Although the vectors does not rotate in a three-phase transformer, for analysis purpose they can be treated as virtual rotating vectors and the sets of switching sequences generate CW and anticlockwise (CCW) rotating vectors across the primary of transformer.

In order to generate high frequency excitation across the primary of the transformer, any two opposite vectors ($\sqrt{3}\vec{V}_0 e^{j(\omega t + \frac{\pi}{6})}$ and $\sqrt{3}\vec{V}_0 e^{j(\omega t + \frac{7\pi}{6})}$) are switched alternatively at high frequency across the transformer. Thus, the line frequency voltage at the utility is amplitude modulated by the high switching frequency of the matrix converter to excite the transformer [22–27]. In ideal transformer with zero leakage, the amplitude modulated voltage is reflected across the secondary winding of the transformer.

Only a single matrix converter MC-3 is connected across the secondary of the transformer and the vectors generated in any sequence are 120° apart [18,20]. Therefore, when the two opposite vectors are reconstructed back by MC-3 two 60° apart separate
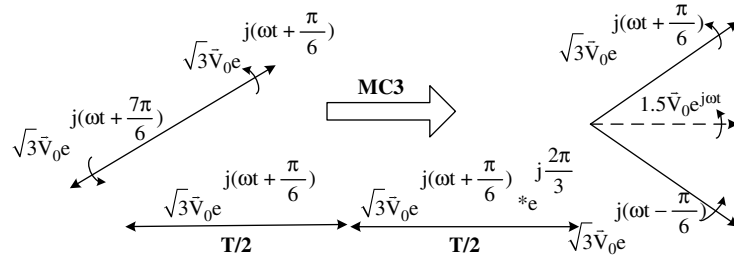
Fig. 15. Any two opposite space vectors and one zero vector is used for voltage synthesis through MC3
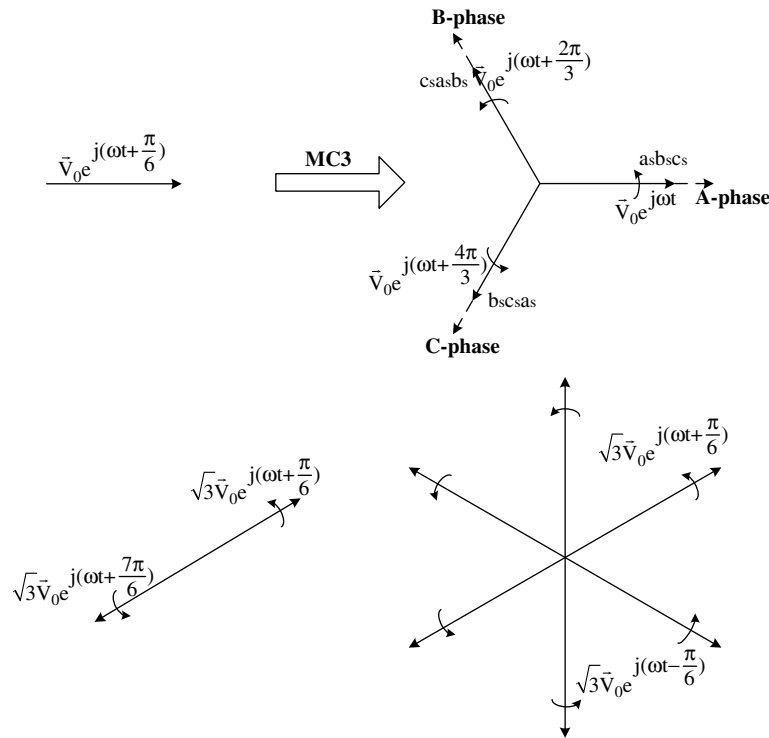

Fig. 16. Any two opposite space vectors and one zero vector is used for voltage synthesis through MC3 in anticlockwise direction

vectors ($\sqrt{3}\vec{V}_0 e^{j(\omega t + \frac{\pi}{6})}$ and $\sqrt{3}\vec{V}_0 e^{j(\omega t - \frac{\pi}{6})}$) are generated at the output (Fig. 15). Because both of the vectors are switched for equal amount of period (T/2), the average output voltage is $1.5\vec{V}_0 e^{j\omega t}$.

However, converter MC-3 can also generate three space vectors, $120°$ apart from a single vector. Referring to Fig. 16, using the switching sequence $a_s b_s c_s$, $c_s a_s b_s$, $b_s c_s a_s$ two opposite vectors would generate six anticlockwise (CCW) rotating vectors $60°$ apart. By using adjacent vectors in Fig. 16, an output vector is synthesized at any desired frequency, amplitude and the direction of rotation, where the maximum achievable amplitude is $(1.5 \times \frac{\sqrt{3}}{2})$ pu. Similarly, output voltage synthesis is possible using CW rotating vectors. The power factor at the input side is controllable by the way described in previous two sections.

8. High Frequency Transformer Link Three-Level Inverter Drive with Common-Mode Voltage Elimination

The topology described in the last section constitutes of large number of switches and suitable for power system application. In application related to drives in wind power it is desirable to have systems with less device count. In wind turbines generally there are large power transformers at the basement and it is preferable to have small high frequency transformers so that it

can be accommodated at the hub near the turbine. It is more suitable to have a single-phase high frequency transformer in place of three-phase one to reduce foot area. Operation of single-phase high frequency transformer are available in literature, and in this section, the application of a matrix converter driven single-phase transformer is applied with common-mode voltage elimination at the three-phase motor load.

The front-end converter as in Fig. 17, first converts the three-phase input AC voltage at the line frequency to DC by creating a virtual DC link. This is called the rectification stage. In the following inversion stage, it converts the virtual DC to a high frequency AC which is fed to the transformer. A three-phase low frequency AC is converted into a high frequency single-phase AC. This converter is basically a direct-link matrix converter with a conventional rectification stage followed by a single-phase inverter instead of a three-phase one. The line currents are also shaped to be in phase with the input voltage waveform.

The PWM signals for the front-end converter are generated using a simple triangle comparison method [9] or any standard techniques available in literature. The link voltage at the output phase A and B, $v_A(t)$ and $v_B(t)$, respectively, are synthesized on an average over a sub-cycle period T_s from $v_a(t)$, $v_b(t)$ and $v_c(t)$. Although the modulation can be realized in many different ways, in the description here the carrier-based modulation technique
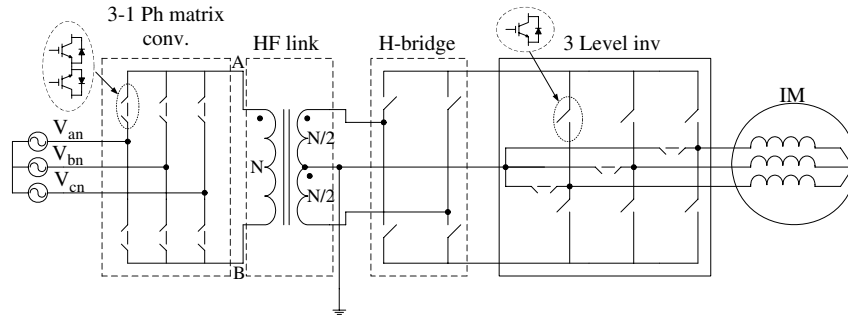
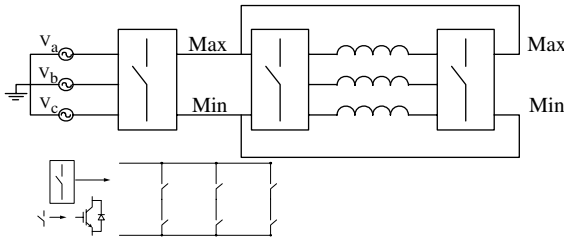Fig. 17. Circuit diagram of the single phase power-electronic transformer

Fig. 18. Direct-link drive for open-end winding AC machines

developed in the first section is extended for modulation of matrix converter. An offset duty ratio

$$[D_a \quad D_b \quad D_c]^T = \begin{matrix} [|0.5\cos(\omega t - \rho)| \; |0.5\cos(\omega t - 2\pi/3 - \rho)| \\ |0.5\cos(\omega t + 2\pi/3 - \rho)|]^T \end{matrix}$$

is used for canceling the negative duty ratios and in order to make the sum of total duty ratios equal to unity at all instant an additional offset duty ratio $\Delta_a(t) = \frac{1-(D_a+D_b+D_c)}{2}$, $\Delta_b(t) = 0$, $\Delta_c(t) = \frac{1-(D_a+D_b+D_c)}{2}$ is added.

At any instant $v_{AB}(t) = \frac{3}{2}v_i(k_A(t) - k_B(t))$ and by making $k_A(t) = -k_B(t)$ and toggling $k_A(t)$ between 0.5 and -0.5 an AC voltage can be generated across the primary of transformer. The AC voltage is generated across the center tapped secondary is rectified through a controlled rectifier. The rectified voltage is acts as three-level voltage for the three-level inverter. The three-level inverter is operated as a two-level inverter in order to eliminate any common-mode voltage in the machine [14]. The switching in the inverter and rectifier and matrix converter are synchronized in order to eliminate any change in voltage levels at the primary of transformer [28].

9. Two-Level Indirect Matrix Converter

Matrix converter driven open-end winding drives described in the previous sections employ 36 unidirectional switches. A direct-link AC–AC power converter utilizing unidirectional switches to drive three-phase star (or delta) connected machines was presented in Ref. [36]. It does not require a DC-link capacitor or input inductors for energy storage. An 18-switch alternative topology (Fig. 18) for open-end winding ac machines [22] is described here. It can generate the same output voltage as generated by the 36-switch counterparts. However, the common-mode voltage at the terminals of the machine is a slowly varying waveform.

The common-mode voltage does not however contain any components at the switching frequency. Considering the low magnitude and frequency of harmonics present in the common-mode voltage, their contribution toward generating bearing currents in the machine will be negligible. In Fig. 19, the front-end converter (RECT) operates like a three-phase diode bridge rectifier and connects the positive terminal (P) of the direct link to the maximum

phase voltage and the negative terminal (N) to the minimum phase voltage.

The direct-link voltage is thus a three-phase line-rectified voltage. The two inverters (INV1 and INV2) modulate the direct-link voltage to generate ac voltage across the machine phase-windings. Detailed operation of the direct-link drive is outlined in (14) and (22). Each inverter has six active vectors and two zero vectors. Three of the six active vectors have a common-mode voltage of $v_d/3$ where v_d is the direct-link voltage. The other three active vectors have a common-mode voltage of $2v_d/3$. If only one of these sets is used by both inverters to generate the voltage across the machine phase windings, the common-mode voltage across the windings is zero and the common-mode voltage at the terminals is either of $v_d/3$ or $2v_d/3$. Also the magnitude of the resultant voltage vectors across the machine phase windings is $\sqrt{3}\,v_d$. Thus, the maximum voltage that can be applied across the machine phase windings is $1.5\,\hat{V}_{in}$ where $\hat{V}_{in}$ is the peak value of the input phase voltage. Owing to the diode bridge rectifier like operation of the front-end rectifier, the input current is a 120°—conduction waveform. The input power factor is not controllable and the input current has considerable total harmonic distortion (THD) ($\approx 30\%$). A solution with multiple drives with phase shifting transformers has been presented in Ref. [22].

10. Unified Two-Level Converter with Power Factor Correction

The direct-link drive described in the previous section has uncontrollable input power factor and poor input current THD. In order to compensate for the input current harmonics, a minimum switch active compensation scheme is proposed in Ref. [37]. The topology for the unified system with active power filtering is shown in Fig. 19. A clamp circuit consisting of a clamp diode D_{cl} and a clamp capacitor C_{cl} (Fig. 19) needs to be used for protection in the direct-link drive and for ride through purpose. The active filter utilizes this clamp capacitor to inject compensating harmoinic currents into the input supply.

For proper operation of the drive, the clamp diode must remain reverse-biased during normal drive operation. The voltage across the clamp capacitor is controlled by the active filter to be higher than the maximum direct-link voltage. Detailed analysis of the unified drive with active filtering is presented in Ref. [37].

The objective of harmonic elimination and power factor correction can also be achieved using a conventional active filter with an isolated capacitor. The essence of the described active filtering mechanism lies in the combination of the active filter with the clamp circuit and still being able to achieve controllable power factor with no input current harmonics.

11. Conclusion

Research on different application of matrix converter undertaken in University of Minnesota is presented. A simplified carrier-based
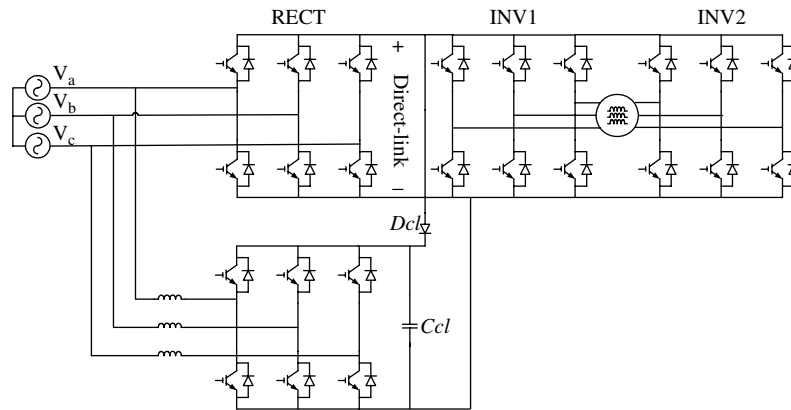
Fig. 19. Unified direct-link drive with active filtering

modulation of matrix converter is derived along with operation for both over-modulation and input unbalance operation. Application of matrix converter for common-mode voltage elimination in open-ended drive is presented. Two possible topologies were discussed along with inherent capability of input power factor control. The input power factor is unity irrespective of output power factor and also the input power factor is controllable. Possible application for high frequency transformer is also discussed. Both single-phase and three-phase topologies for high frequency transformer application were proposed.

Acknowledgements

References

(1) Gyugyi LG, Pelly, BR. *Static Power Frequency Changers, Theory, Performance, and Applications*. John Wiley & Sons: New York; 1976; 442.

(2) Wood P. *Switching Power Converters*. Van Nostrand Reinhold Co.: New York, c 1981. 446 ISBN: 0442243332.

(3) Alesina A, Venturini M. Analysis and design of optimum amplitude nine-switch direct AC-AC converters. *IEEE Transactions on Power Electronics* 1989; **4(1)**:101–112.

(4) Wheeler PW, Rodriguez J, Clare JC, Empringham L. Matrix converter, A technology review. *IEEE Transactions on Industrial Electronics* 2002; **49(2)**:276–288.

(5) Kolar JW, Schafmeister F, Round SD, Ertl H. Novel three-phase AC–AC sparse matrix converters. *IEEE Transactions on Power Electronics* 2007; **22(5)**:1649–1661.

(6) Huber L, Borojevic D. Space vector modulated three-phase to three phase matrix converter with input power factor correction. *IEEE Transactions on Industrial Applications* 1995; **31(6)**:1234–1246.

(7) Helle L, Larsen KB, Jorgensen AH, Munk-Nielsen S, Blaabjerg F. Evaluation of modulation schemes for three-phase to three-phase matrix converters. *IEEE Transactions on Industrial Electronics* 2004; **51(1)**:158–171.

(8) Oyama J, Higuchi T, Yamada E, Koga T, Lipo T. New control strategy for matrix converter. *Conference Record IEEE PESC*, June 1989; 360–367.

(9) Mohan N, Mohapatra KK, Jose P, Drolia A, Aggarwal G, Satish T. A novel carrier based PWM scheme for matrix converters that is easy to implement. *Conference Record of PESC* 2005; 2410–2414.

(10) Satish T, Mohapatra KK, Mohan N. Modulation methods based on a novel carrier-based PWM scheme for matrix converter operation under unbalanced input voltages. *Applied Power Electronics Conference and Exposition, 2006. APEC '06. Twenty-First Annual IEEE*, 19–23 March 2006; 127–132.

(11) Satish T, Mohapatra KK, Mohan N. Steady state over-modulation of matrix converter using simplified carrier based control. *Industrial Electronics Society, 2007. IECON 2007. 33rd Annual Conference of the IEEE*, 5–8 November 2007; 1817–1822.

(12) Shivakumar EG, Gopakumar K, Ranganathan, VT. Space vector PWM control of dual inverter fed open-end winding induction motor drive. *IEEE-APEC,* 2000; 394–404.

(13) Stemmler H, Guggenbach P. Configurations of high power voltage source inverter drives *Proceedings of EPE'93 Conference*, Brighton, UK, 1993; 7–12.

(14) Baiju MR, Mohapatra KK, Kanchan RS, Gopakumar K. A dual two-level inverter scheme with common mode voltage elimination for an induction motor drive. *IEEE Transaction on Power Electronics* 2004; **19(3)**:794–805.

(15) Somasekhar VT, Gopakumar K, Baiju MR, Mohapatra KK, Umanand L. A multilevel inverter system for an induction motor with open-end windings. *IEEE Transactions on Industrial Electronics* 2005; **52(3)**:824–836.

(16) Braun, M, Hasse, K. A direct frequency changer with control of input reactive power. *IFAC Control in Power Electronics and Electrical Drives*, Lausanne, Switzerland, 1983; 187–194.

(17) Ma X. High performance PWM frequency changers. *IEEE Transactions on Industry Applications* 1986; **IA-22**:267–280.

(18) Mohapatra KK, Mohan N. Open-end winding induction motor driven with matrix converter for common-mode elimination. *Power Electronics, Drives and Energy Systems, 2006. PEDES '06. International Conference*, 12–15 December 2006; 1–6.

(19) Rzasa J. Control of a Matrix Converter with Reduction of a common mode voltage, *Conference Record of Compatibility in Power Electronics*, 1 June 2005; 213–217.

(20) Mohapatra KK, Mohan N. Open-end winding induction motor driven with indirect matrix converter for common-mode elimination. *SCSC: Proceedings of the 2007 Summer Computer Simulation Conference*, San Diego, California, 2007; 106–111.

(21) Somani A, Gupta RK, Satish T, Mohapatra, KK. A PEBB-based direct-link drive for open-ended AC machines. *Proceedings of the 2007 Summer Computer Simulation Conference*, San Diego, California, 2007; 118–123.

(22) Kang M, Enjeti PN, Pitel IJ. Analysis and design of electronic transformers for electric power distribution system. *IEEE Transactions on Power Electronics* 1999; **14(6)**:1133–1141.

(23) Cha H, Enjeti P. A three-phase ac/ac high frequency link matrix converter for vscf applications. *PESC*, 15–19 June 2003, vol **4**; 1971–1976.

(24) Ronan ER, Sudhoff SD, Glover SF, Galloway DL. A power electronic-based distribution transformer. *IEEE Transactions on Power Delivery* 2002; **17**:537–543.

(25) Manjrekar MD, Kieferndorf R, Venkataramanan G. Power electronic transformers for utility applications. *Industry Applications Conference, 2000. Conference Record of the 2000 IEEE*, 8–12 October 2000, vol. 4; 2496–2502.

(26) Krishnaswami H, Ramanarayanan V. Control of high-frequency AC link electronic transformer. *IEE Proceeding -Electric Power Applications* 2005; **152(3)**:509–516.

(27) Jin Aijuan, Li Hangtian, Li Shaolong. A three-phase four-wire high-frequency AC link matrix converter for power electronic transformer. *Electrical Machines and Systems, 2005. ICEMS 2005. Proceedings of the Eighth International Conference on*, 27–29 September 2005; vol. 2, 1295–1300.

(28) Basu K, Umarikar A, Mohapatra KK, Mohan N. High frequency transformer link three level inverter drive with common mode voltage elimination. *Conference Record of PESC'08* (accepted for publication).

(29) KK Mohapatra, Mohan N. Matrix converter fed open-ended power electronic transformer for power system application. Accepted for publication in *IEEE Power Engineering Society General Meeting*, Pittsburgh, 2008.

(30) Rodriguez J, Lai Jih-Sheng, Peng FangZheng. Multilevel inverters: a survey of topologies, controls, and applications. *IEEE Transactions on Industrial Electronics* 2002; **49**(4):724–738.

(31) Hava AM, Kerkman RJ, Lipo TA. Carrier-based PWM-VSI overmodulation strategies: Analysis, comparison and design. *IEEE Transactions on Power Electronics* 1998; **13**(4):674–689.

(32) Zhou D, Sun K, Huang L. Evaluation of matrix converter operation in abnormal conditions *Conference Record IEEE, ICEMS'03*, 2003; 402–406.

(33) Casadei D, Serra G, Tani A. Reduction of the input currents harmonic content in matrix converters under input/output unbalance. *IEEE Transactions on Industrial Electronics* 1998; **45**(3):401–411.

(34) Casadei D, Serra G, Tani A. A general approach for the analysis of input power quality in matrix converters. *IEEE Transactions on Power Electronics* 1998; **13**(5):882–891.

(35) Vincenti. D, Jin H, A generalized approach for input unbalance correction in polyphase PWM converters *Proceedings of IEEE IECON'95*, vol. 1; 365–369.

(36) Kim S, Sul S-K, Lipo TA. AC/AC power conversion based on matrix converter topology with unidirectional switches. *IEEE Transaction on Industry Applications* 2000; **36**(1):139–145.

(37) Somani A, Gupta R, Mohapatra KK, Mohan N. A minimum-switch direct-link drive with common-mode voltage suppression and active filtering for open-end winding AC machines *IEEE, Power Electronics Specialists Conference (PESC)*, Greece, 2008; 2889–2893.

(38) Mohapatra KK, Mohan N. Open-ended control circuit for electrical apparatus. *Intellectual Property Protection Application by the University of Minnesota*, 2007.

Krushna K. Mohapatra (Non-member) received a Ph.D. degree from the Indian Institute of Science, Bangalore, India, in 2004. He is currently a Research Associate in the Electrical Engineering Department at the University of Minnesota, Minneapolis, USA. His research interests are in the area of power converters, PWM strategies, and motor drives.

Ranjan K. Gupta (Non-member) is a Ph.D. student in the Department of Electrical and Computer Engineering at the University of Minnesota, Minneapolis. He completed his Bachelor degree in Electrical Engineering from Indian Institute of Technology Roorkee in 2004. His research interests are in the area of electrical machine design and electric drives.

Satish Thuta (Non-member) received a Ph.D. in Electrical Engineering from University of Minnesota, Minneapolis, USA, in 2007. Currently he is with R&D Division, Ford Motors Dearborn, MI, USA. His research interests include power electronics, motor drives, PWM techniques, switch mode power supplies and control systems.

Apurva Somani (Non-member) received his bachelor's degree in Electrical Engineering in 2006 from Indian Institute of Technology Kanpur. Currently he is pursuing graduate studies in Electrical Engineering at the University of Minnesota. His research interests are in the areas of power electronics and electric drives.

Amod Umarikar (Non-member) received his doctoral degree in Electrical Engineering in 2006 from Indian Institute of Science, Bangalore. Currently he is a postdoctoral associate in the department of Electrical Engineering, University of Minnesota, Minneapolis, USA. His research interests are modeling and simulation of power electronic systems and electric drives.

Kaushik Basu (Non-member) received the M.Sc. (Engg) degree from Indian Institute of Science, Bangalore, India, in 2005 in Electrical Engineering. He is currently pursuing Ph.D. degree in Electrical Engineering at the University of Minnesota, Twin Cities, USA. His major research interests are PWM techniques, motor drives and magnetics design.

Ned Mohan (Non-member) is the Oscar A. Schott professor of power electronics at the University of Minnesota, Minneapolis, where he has been teaching since 1976. He has numerous patents and publications in the field of power electronics, electric drive and power systems. He has written five textbooks. Prof. Mohan is a recipient of the Distinguished Teaching Award presented by the Institute of Technology, University of Minnesota. He received the Morse-Alumni Distinguished Teaching Award from the University of Minnesota, and the 2008 Outstanding Power Engineering Educator Award from the IEEE-PES. He is a Fellow of the IEEE.